Received: 21 December 2016 | Revised: 1 August 2017 | Accepted: 6 August 2017

DOI: 10.1111/geb.12639

RESEARCH PAPER

WILEY Global Ecology and Biogeography A Journal of Macroecology

Spatial heterogeneity of biomass and forest structure of the Amazon rain forest: Linking remote sensing, forest modelling and field inventory

Edna Rödig[1,2] | Matthias Cuntz[2,3] | Jens Heinke[4] | Anja Rammig[4,5] | Andreas Huth[1,6,7]

[1]Department Ecological Modelling, Helmholtz Centre for Environmental Research (UFZ), Leipzig, Germany

[2]Department Computational Hydrosystems, Helmholtz Centre for Environmental Research (UFZ), Leipzig, Germany

[3]Institut National de la Recherche Agronomique (INRA), Universite de Lorraine, UMR1137, Ecologie et Ecophysiologie Forestières, Champenoux, France

[4]Potsdam-Institute for Climate Impact Research (PIK), Earth System Analysis, Potsdam, Germany

[5]Technical University of Munich (TUM), School of Life Sciences Weihenstephan, Freising, Germany

[6]Institute of Environmental Systems Research, University of Osnabrück, Osnabrück, Germany

[7]German Centre for Integrative Biodiversity Research (iDiv) Halle-Jena-Leipzig, Leipzig, Germany

Correspondence
Edna Rödig, Helmholtz Centre for Environmental Research (UFZ), Leipzig, Germany.
Email: edna.roedig@ufz.de

Funding information
Helmholtz-Alliance Remote Sensing and Earth System Dynamics; Helmholtz Impulse and Networking Fund

Abstract

Aim: Estimating the current spatial variation of biomass in the Amazon rain forest is a challenge and remains a source of substantial uncertainty in the assessment of the global carbon cycle. Precise estimates need to consider small-scale variations of forest structures resulting from local disturbances, on the one hand, and require large-scale information on the state of the forest that can be detected by remote sensing, on the other hand. In this study, we introduce a novel method that links a forest gap model and a canopy height map to derive the biomass distribution of the Amazon rain forest.

Location: Amazon rain forest.

Methods: An individual-based forest model was applied to estimate the variation of aboveground biomass across the Amazon rain forest. The forest model simulated individual trees; hence, it allowed the direct comparison of simulated and observed canopy heights from remote sensing. The comparison enabled the detection of disturbed forest states and the derivation of a simulation-based biomass map at 0.16 ha resolution.

Results: Simulated biomass values ranged from 20 to 490 t (dry mass)/ha across 7.8 Mio km^2 of Amazon rain forest. We estimated a total aboveground biomass stock of 76 GtC, with a coefficient of variation of 45%. We found mean differences of only 15% when comparing biomass values of the map with 114 field inventories. The forest model enables the derivation of additional estimates, such as basal area and stem density.

Main conclusions: Linking a canopy height map with an individual-based forest model captures the spatial variation of biomass in the Amazon rain forest at high resolution. The study demonstrates how this linkage allows for quantifying the spatial variation in forest structure caused by tree-level to regional-scale disturbances. It thus provides a basis for large-scale analyses on the heterogeneous structure of tropical forests and their carbon cycle.

KEYWORDS
Amazonia, biomass, forest gap model, mortality rates, remote sensing, tropical forests

1 | INTRODUCTION

Observing the dynamics of terrestrial biomass is a great challenge and one of the major sources of uncertainties in the global carbon cycle (Le Quéré et al., 2016). In particular, tropical forests are sensitive to anthropogenic disturbances, such as deforestation or logging, that cause large-scale forest degradation (van der Werf et al., 2009). The Amazon rain forest is the largest intact tropical forest, with a share of *c.* 18% of global forest area (Hansen, Stehman, & Potapov, 2010). Robust estimates of its aboveground biomass (AGB) and forest structure are essential to correctly budget carbon emissions. However, AGB estimates diverge by a factor of two for the Amazon rain forest,

ranging from 38.9 to 93 PgC (Houghton, Lawrence, Hackler, & Brown, 2001; Malhi et al., 2006; Saatchi, Houghton, Dos Santos Alvalá, Soares, & Yu , 2007; Saatchi et al., 2011).

The large spread of the AGB estimates arises from diverse methodological approaches at different spatial and temporal scales: ground-based measurements, remote sensing, a combination of both, and modelling. On the one hand, ground-based measurements (forest inventories that are mostly at the plot scale of *c*. 1 ha and census intervals of 1 year or more) are interpolated in order to display the spatial distribution of biomass (Johnson et al., 2016; Malhi et al., 2006). As the number of observations is limited, it is uncertain how representative these samples are for the whole basin (Chave et al., 2004; Marvin et al., 2014; Réjou-Méchain et al., 2014). Therefore, ground-based measurements are often linked with remote sensing products that capture the state of forests, in order to derive static maps of AGB (e.g., 1 km^2 resolution in Avitabile et al., 2016; Saatchi et al., 2011). On the other hand, modelling approaches, such as dynamic global vegetation models (DGVMs), simulate the temporal dynamics of biomass at regional scales (e.g., Sitch et al., 2003). Such models are applied, for example, for investigating the impact of climate change on Amazon rain forest ecosystems (e.g., Huntingford et al., 2008; Rammig et al., 2010) and can be useful to provide hypotheses for the underlying mechanisms that drive biomass distribution and dynamics (e.g., Hofhansl et al., 2016). Depending on the resolution of the climate input, these models mostly cover large-scale patterns of mature forests at a spatial resolution of > 10 km^2. Thus, they may not capture forest structures and dynamics at small scales, such as the individual tree level and effects of logging. This may be a reason for the divergence (Johnson et al., 2016) from maps that combine remote sensing and ground observations (Avitabile et al., 2016; Baccini et al., 2012; Saatchi et al., 2011).

There is clearly a need for the combination of remote sensing products and vegetation models in order to broaden our knowledge on the dynamics, structures and carbon stocks in the Amazon rain forest. Here, we present a method to bridge this gap by linking remote sensing data with an individual-based forest gap model (FORMIND; Fischer et al., 2016; Köhler & Huth, 2004).

Individual-based forest gap models are normally applied at the local scale to reproduce successional dynamics and forest structures (e.g., Botkin, Janak, & Wallis, 1972; Bugmann, 2001; Shugart, 1984; Shugart et al., 2015). In contrast to DGVMs, forest gap models simulate processes of tree growth, establishment and mortality for each tree individually. This concept enables the projection of forest succession, vertical and horizontal heterogeneity, competition between individuals, and disturbances owing to stem-based mortality. Individual-based forest models thereby depict forest structure more closely than area-based models (Smith, Prentice, & Sykes, 2001).

In the present study, we expand the forest gap model FORMIND from the local scale (stand level) to the regional scale (entire Amazon rain forest). This regionalization implies some model adaptations. First, we adapt the model's mortality parameters that influence simulated tree species composition across the Amazon. We find that annual precipitation and clay fraction are a potential proxy for tree mortality rates in our forest model. This relationship is supported by observations made in the field (Galbraith et al., 2013; Malhi et al., 2015; Quesada et al., 2012). The adapted individual-based forest gap model is then applied across the Amazon to simulate all potential successional stages and related tree heights.

Second, we assume that canopy height is a good indicator for the successional stage of a forest site (Dubayah et al., 2010). We use remotely sensed canopy heights from a high-resolution (1 km^2) wall-to-wall map derived from spaceborne light detection and ranging (LIDAR; Simard, Pinto, Fisher, & Baccini, 2011) as a proxy for the successional state of the forest (inspired by Hurtt et al., 2004; Ranson et al., 2001). We then link the observed with the simulated canopy height and successional stage of our forest gap model to derive the amount of AGB stored at each location. Combining both tools results in a new, high-resolution, simulation-based AGB map of the Amazon rain forest that takes natural and anthropogenic disturbances into account.

The following research questions will guide us through the study.

1. What is the benefit of linking remote sensing data and a forest model?
2. How well does simulated AGB represent ground observations?
3. How does forest structure influence the spatial distribution of AGB in the Amazon rain forest?

2 | METHODS

2.1 | The individual-based forest gap model

The individual-based, forest gap model FORMIND (Fischer et al., 2016; Köhler & Huth, 2004) was developed specifically for the simulation of tropical forests. Tree species are assigned to plant functional types (PFTs) in order to represent forests of high diversity. Forests can thereby develop through different successional stages. In FORMIND, tree growth is mainly driven by light (photosynthetic photon flux density (PPFD)). Four main processes are calculated for each tree individually in each time step: establishment, competition for light, growth and mortality (Figure 1; for more details see Supporting Information Appendix Figure S1). An individual tree can establish if there is sufficient space and light. As trees grow individually in the model, each tree competes for space and light. Tree growth results from its carbon balance, including photosynthetic production and respiratory losses. Mortality of a tree depends on stem diameter and is determined stochastically. The forest site is divided into 20 m $\times$ 20 m patches ('gaps'). Within each patch, trees have no explicit position.

As a first step, FORMIND was applied to local forest stands in central Amazon where detailed forest inventory data were available (stem size distributions of different successional stages in the Amazon basin, Brondizio & Moran, 2009; in climax stage near Manaus, Kunert, Aparecido, Higuchi, Santos, & Dos Trumbore, 2015). Species were assigned to three plant functional types (early, mid and late successional trees). FORMIND was found to reproduce observed biomass and stem size distributions of the

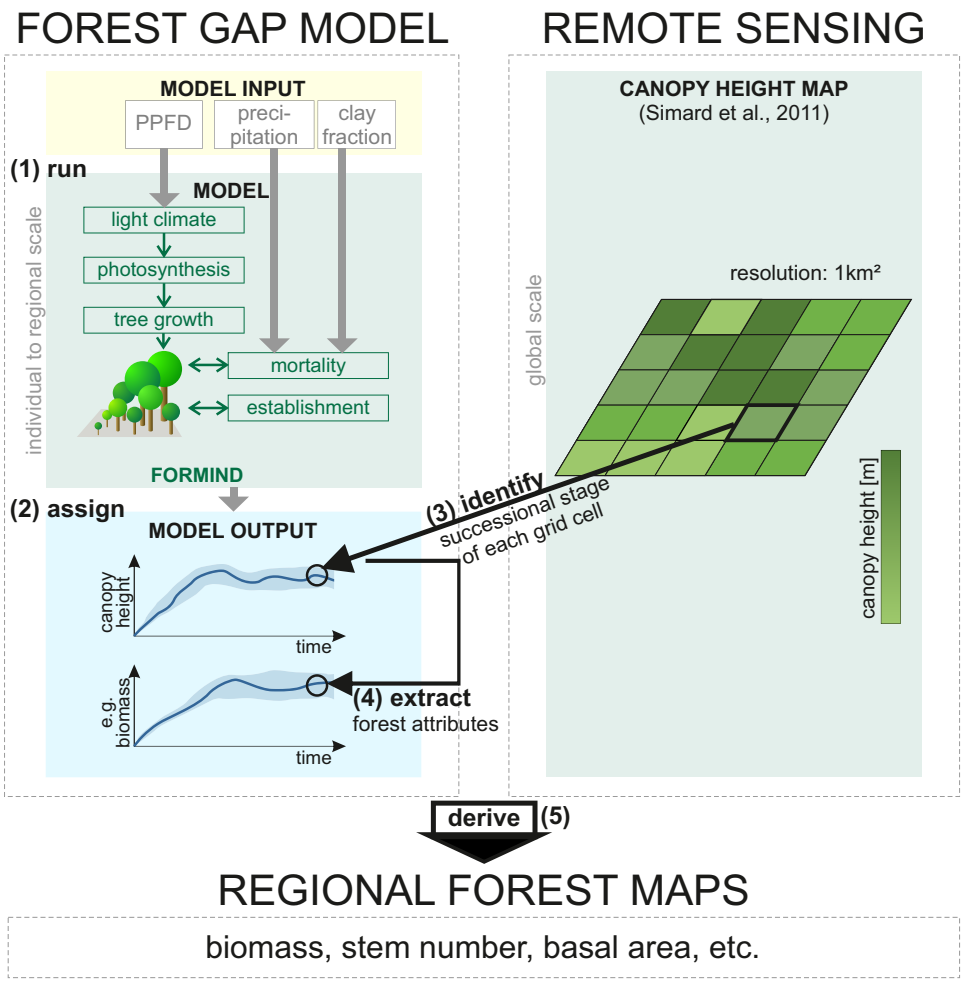

FIGURE 1 The five working steps to derive regional maps from an individual-based forest gap model in combination with remote sensing data: (1) run the forest model on 1km^2 to equilibrium driven by local photosynthetic photon flux density (PPFD), precipitation and clay fraction, (2) assign the simulations to the grid cells of the Amazon rainforest according to similar input, (3) link canopy height of remote sensing data at each location with the forest simulations to identify the successional stage, (4) extract other simulated forest attributes at the same successional state (e.g., above-ground biomass). (2)-(3) is performed for every 1km^2 grid cell within the Amazon rainforest to finally (5) derive forest maps.

different successional states (see Supporting Information Appendix S1.2 and Figure S2 for parameterization of the basic forest model).

2.2 | The regional individual-based forest gap model

Expanding the forest model from the local scale (stand level) to the regional scale (entire Amazon rain forest) implied some model adaptations. Preliminary tests showed that driving the model by spatially variable PPFD (WFDEI Forcing Data; Weedon et al., 2014) alone is not sufficient to reproduce different species (here PFTs) compositions across the Amazon rain forest. Supported by literature (Castanho et al., 2013; Galbraith et al., 2013; Malhi et al., 2015), we found that we can adapt the forest model's mortality parameter of shade tolerant, late successional trees to match inventory data better. This key parameter was calibrated (Lehmann & Huth, 2015; see Supporting Information Appendix S1.3 for calibration method and objective function) to simulate aboveground forest biomass, mean wood density and basal area information of 180 sites with mature forest (Lopez-Gonzalez, Lewis, Burkitt, & Phillips, 2014; Mitchard et al., 2014). The mortality rate of the shade tolerant species (PFT3) was the most dominant driver for structural differences, so we calibrated only this mortality parameter to simplify the procedure, following Occam's razor. The calibration resulted in 180 different parameter sets (one mortality parameter for PFT3 (late successional trees) per site).

The calibrated mortality parameters were correlated with local characteristics such as climatic conditions (precipitation, length of dry season and climatic water deficit) and soil properties (classification and chemical properties), which were derived from global maps (Supporting Information Table S6). We investigated linear (Supporting Information Table S4) and multivariate (Supporting Information Table S5) linear regressions between calibrated parameters and 40 local conditions. The calibrated mortality parameters were best replicable with a linear function driven by precipitation and clay fraction (as a representative for soil type). This relationship is supported by field observations, which state that tree mortality may be related to drought characteristics (Malhi et al., 2015) and soil physical properties (Quesada et al., 2012).

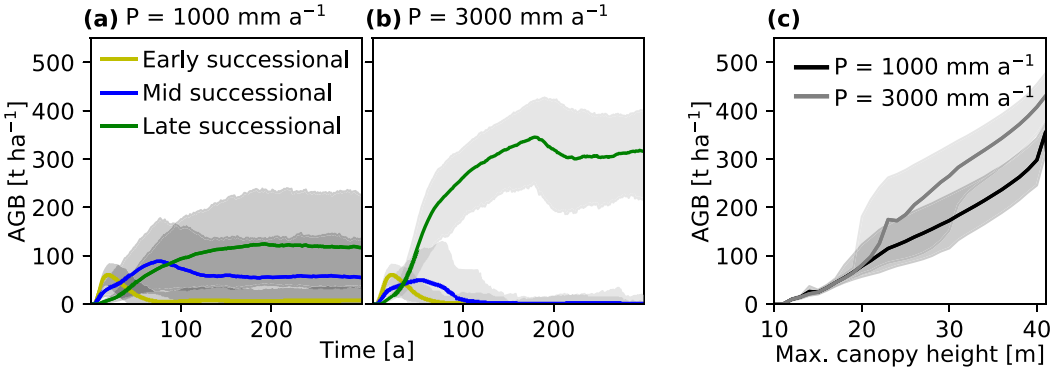

FIGURE 2 (a,b) Exemplary, mean above-ground biomass (AGB) of 1 km^2 over time (solid lines) for the three plant functional types (early, mid and late successional trees) from 'bare ground' to climax stage for: (a) annual precipitation (P) of 1000 m a-1, clay fraction of 30% and photosynthetic photon flux density PPFD = 720 μmol m-2 ha-1, (b) annual precipitation of 3000 m a-1, clay fraction = 30% and PPFD = 720 μmol m-2 ha-1. Mortality is driven by precipitation and clay fraction which results in different forest structures. The shaded range around mean AGB shows the spatial variation (95% quantile) of 100 ha plots (100 individual 1 ha plots in 1 km^2). (c) Total AGB of all 40 m × 40 m plots within 1 km^2 (simulation time of 1000 years) over its maximum canopy height, exemplary for two response units. The shaded range around AGB results from the different time steps when the maximum canopy height is reached.

Note that the analysis was restricted to climatic and soil conditions that were available as Amazon-wide, continuous maps. Nutrients in soils were not considered in the analysis. FORMIND was extended by the input annual precipitation (derived from WFDEI; Weedon et al., 2014) and clay fraction (Wieder, Boehnert, Bonan, & Langseth, 2014) as a proxy for mortality. Mortality is reduced with rising precipitation and clay fraction (see Supporting Information Appendix S1.3 for function and parameter values). Our regionalization method was inspired by regionalization techniques commonly used in hydrology, where model parameters are linked with land surface properties (Blöschl & Sivapalan, 1995; Samaniego, Kumar, & Attinger, 2010).

2.3 | Large-scale simulations of the Amazon rain forest

We applied the adapted forest model on the entire Amazon rain forest as defined by the following criteria (as in Malhi et al., 2006): all forest plots are located at an elevation < 1,000 m; they are categorized as rain forest or moist deciduous rain forest (according to the Food and Agriculture Organization definition) and have an annual mean temperature > 18 °C. In this study, we considered additionally only forest plots that have a mean maximal canopy height > 10 m. Global and regional datasets (climate, soil properties, canopy height map; Supporting Information Table S6) used in this study were processed with the Climate Data Operators (CDO, 2015).

In order to reduce computational effort, we classified the Amazon rain forest into areas of similar environmental conditions, as follows: mean annual precipitation (eight classes [0–500, 500–1,000, …, 3,500–4,000] in millimetres per annum), clay fraction (10 classes [0–0.1, 0.1–0.2, …, 0.9–1]) and mean annual PPFD (16 classes [670–690, 690–710, …, 970–990] in micromoles per square metre per hectare). This resulted in 1,280 areas in total, which we refer to as 'response units' (Supporting Information Figure S2). The assumption is that forest dynamics are similar within each response unit because of similar input conditions (inspired by the concept of 'hydrological response units' in Flügel, 1995). FORMIND was used to simulate forest succession from bare ground to climax stage over 1,000 years on an area of 1 km^2 (100 ha) for each response unit. In total, we simulated growth of more than 50 Mio individual trees (stem diameter ≥ 10 cm) spread over 1,280 km^2 of forest. The calculations were performed in parallel (per 1 km^2) on a Linux-based computer cluster (simulation time- < 20 min on 1,000 cores). According to local environmental and soil conditions, we assigned the simulation results of the response units to each 1 km^2 grid cell of the Amazon rain forest.

2.4 | Linking remote sensing data and the forest gap model to identify forest successional states

After 300–500 years of simulation, the simulated forests in all regions within the Amazon rain forest reach climax stage, where dynamics are driven by tree mortality caused by tree fall or crowding. In the following, we refer to simulations in climax stage as the 'undisturbed scenario'. We linked our simulation results and a wall-to-wall canopy height map (Simard et al., 2011) in order to identify the actual successional state of forests caused by larger disturbances such as logging, deforestation or blow-downs (Figure 1). The canopy height map was derived from remotely sensed LIDAR data (2005 data from the Geoscience Laser Altimeter System (GLAS)) and has a resolution of 1 km^2.

For each grid cell, we identified the time steps (within simulation years 0–1,000) of the forest simulation when simulated canopy height was equal to the observed, static value of the canopy height map. The simulations then provided additional forest attributes at the identified time steps, such as AGB (Figure 2c), basal area or tree density. It is therefore possible to derive regional maps of, for example, AGB for the Amazon rain forest. In the following, we refer to this simulation as the 'disturbed scenario'. The 'disturbed scenario' describes the current state of the Amazon, whereas the 'undisturbed scenario' describes the potential biomass of the Amazon under current mean climate

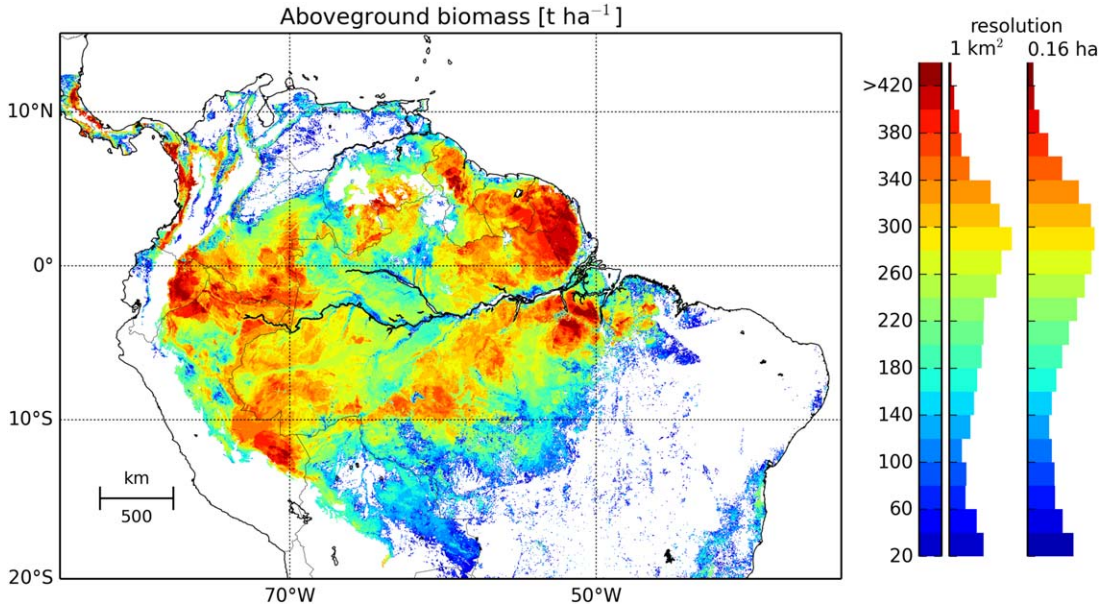

FIGURE 3 Map (left) of aboveground biomass (stem diameter > 10 cm) in the Amazon rain forest (South American rain forest with elevation < 1,000 m) and relative frequency distributions (right) at 1 km^2 resolution and at 40 m × 40 m resolution (smallest resolution of forest model) simulated with an individual-based forest model. Successional stages within the simulation were identified via a canopy height map

(Supporting Information Figure S3). The potential biomass of the 'undisturbed scenario' is derived by calculating the mean biomass over years 500–1,000 of the simulation (forest in mature state). We also tested a model version for which we hold the mortality rates constant throughout the entire Amazon rain forest, which we refer to as the 'disturbed scenario with constant mortality'.

2.5 | Spatial resolution of the approach

The highest resolution in our approach is the individual tree that grows within a 20 m × 20 m patch. This patch is aggregated to 40 m × 40 m (2 × 2 patches, 0.16 ha) in order to mimic the footprint of a GLAS shot (Supporting Information Figure S4). From this, we can derive frequency distributions for AGB for the Amazon at different spatial resolutions. In this study, we focus on the 0.16 ha scale (scale of GLAS footprint) and the 1 km^2 scale (scale of canopy height map). The derived AGB map is shown at 1 km^2 resolution, which corresponds to the resolution of the remotely sensed canopy height map. Hence, it represents the simulated AGB values at 1 km^2 resolution by taking the mean over all 40 m × 40 m patches (625 patches, which correspond to 100 ha = 1 km^2). The greatest challenge lies in identifying how the canopy height map values correspond to the simulated canopy height. As the canopy height map was validated with the three tallest trees in a 20 m radius (approximately size of footprint of the LIDAR) by Simard et al. (2011), we assume that the value of the canopy height map corresponds to the simulated mean height of the three tallest trees within 40 m × 40 m.

2.6 | Comparison with field data

The AGB map was compared with field inventories in different successional states. AGB values for stands with mainly mature forest were taken from Houghton et al. (2001) (21 sites, 0.5–50 ha), Mitchard et al. (2014) and Lopez-Gonzalez et al. (2014) (186 sites, 0.25–5 ha, only the ones independent from validation), AGB values for stands with secondary forest from Poorter et al. (2015) (54 sites, 0.3–5 ha). One data set (Lopez-Gonzalez et al., 2014; Mitchard et al., 2014) including 186 sites (0.25–5 ha, only the ones indepedent from validation) was available for the comparison of simulated against observed basal area covering mainly stands with mature forest.

3 | RESULTS

The individual-based forest gap model enabled the simulation of forest dynamics and succession over time. Different environmental conditions have an influence on tree mortality rates. This causes different species compositions across the Amazon rain forest, which can be represented by the ratio between early, mid and late successional trees (Figure 2a, b). In the simulations, late successional trees clearly dominate the forest in regions of high precipitation/clay fraction, whereas species composition is more balanced in regions of lower precipitation/clay fraction.

Linking simulated data with the canopy height map of Simard et al. (2011) resulted in an AGB map at 0.16 ha and 1 km^2 resolution (Figure 3; coefficient of variation in Supporting Information Figure S5). The mean simulated AGB (dry mass) stored in South American tropical rain forests (elevation < 1,000 m) is 222 t/ha; in total 76 PgC on 7.8 Mio km^2. Our AGB map (Figure 3) shows a pronounced gradient between regions of high biomass density in northeastern Amazonia and lower biomass density in southern Amazonia. Highest values are estimated for the north-eastern Guiana Shield and around the east Amazon delta, with AGB up to 490 t/ha. AGB is slightly lower in the central Amazon rain forest along the Amazon river. In western Amazon,

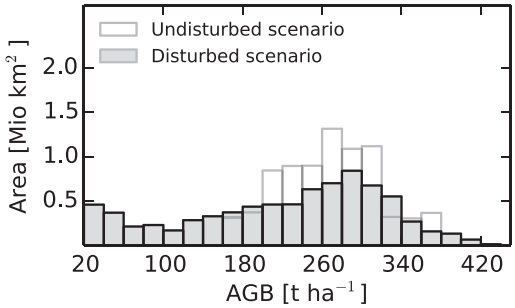

FIGURE 4 Frequency distribution of simulated aboveground biomass (AGB) for the simulated undisturbed scenario (mature forests, steady state of simulations) and disturbed scenario (linked to canopy height map).

biomass distribution varies strongly, with peaks of up to 440 t/ha. At the northern and southern edges, biomass is reduced because of deforestation. We estimated mean AGB values (and *SD*) for four regions across the Amazon basin (regions according to Feldpausch et al., 2011), as follows: Western Amazon 239 ± 99 t/ha, Brazilian Shield 170 ± 102 t/ha, East Central Amazon 226 ± 77 t/ha and Guiana Shield 264 ± 82 t/ha.

Our AGB map considers human-induced and natural disturbances identified via canopy heights. Across the Amazon basin, biomass ranges from 20 to 490 t/ha (mean 222 t/ha with an *SD* of 100 t/ha). If we do not relate the canopy height map to our simulation results, we analyse the simulated forest in an undisturbed, mature state (Figure 4; 'undisturbed scenario', see Methods for details). In this scenario, mean

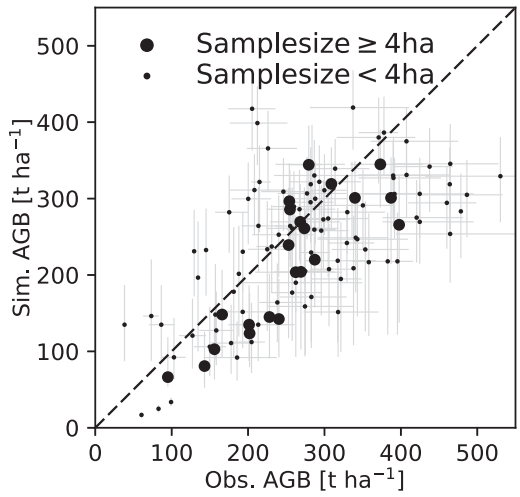

FIGURE 5 Comparison of simulated above-ground biomass (AGB, closest location to inventory in AGB map, Fig. 3) and observed AGB at 114 field inventories (Houghton et al., 2001; Lopez-Gonzalez et al., 2011; Mitchard et al., 2014; Poorter et al., 2015). The ranges of observed AGB (horizontal grey error bars) come from different allometries used in Mitchard et al. (2014). The error bars for the simulated biomass (vertical grey error bars) result from different time steps at which the observed canopy height matches the simulated canopy height. The dashed line is the 1:1 line. R^2 = 0.41; root mean square error (RMSE) and normalized (nRMSE) for samples of sizes >4ha and for all points: $RMSE_{samplesize>4ha}$ = 61 t/ha, $nRMSE_{samplesize>4ha}$ = 0.12, $RMSE_{all}$ = 73 t/ha, $nRMSE_{all}$ = 0.15.

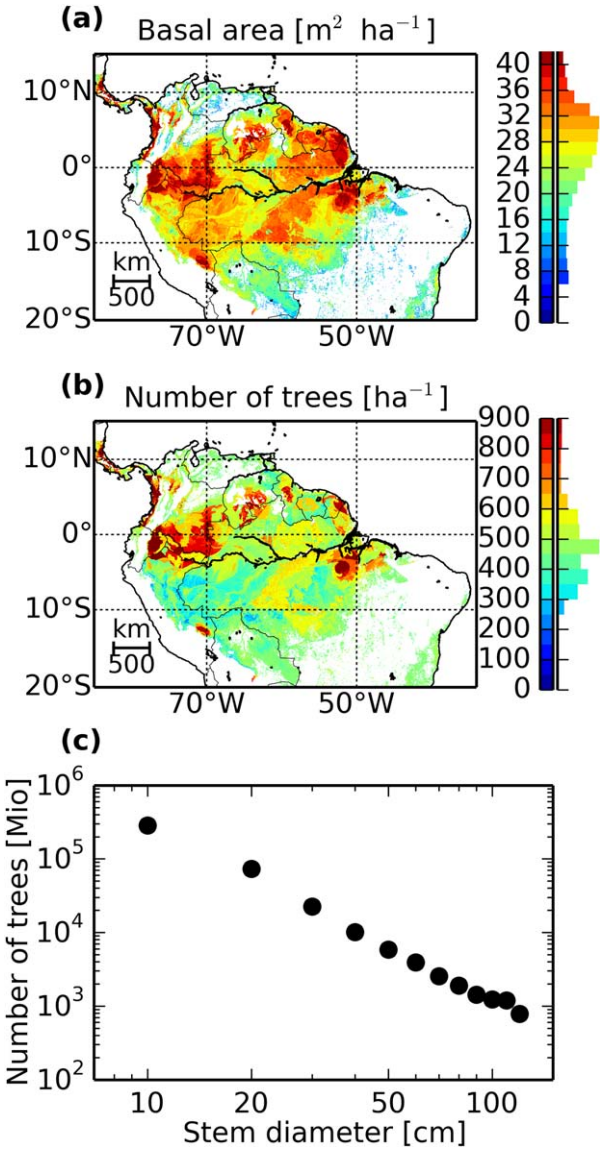

FIGURE 6 Maps (left) and relative frequency distributions (right) of (a) basal area (in square metres per hectare) and (b) number of stems (per hectare; stem diameter > 10 cm) simulated for the Amazon rain forest (elevation <1,000 m) with the forest model linked to a canopy height map. (c) Stem diameter distribution of the entire Amazon rain forest on a log–log scale.

biomass is higher, at 264 t/ha, and the variability of biomass is lower, with an *SD* of 54 t/ha, because natural (e.g. flooding) or anthropogenic disturbances are not considered. In the undisturbed case, total AGB is 15 PgC higher than in the disturbed scenario.

The new AGB map was tested with observed biomass from field inventories (Houghton et al., 2001; Lopez-Gonzalez et al., 2014; Mitchard et al., 2014; Poorter et al., 2015). On average, our model approach underestimates observed biomass by *c.* 15% (R^2 = 0.41). If several inventories were located within one grid cell (1 km^2) they were summed up to larger sample sizes. Note that these samples are not necessarily connected to each other. Values of sample sizes > 4 ha (suggested size of field calibration plots in Réjou-Méchain et al., 2014) match particularly well with a root mean square error (RMSE)

$RMSE_{samplesize>4\,ha} = 61$ t/ha (normalized $RMSE_{samplesize\,>\,4\,ha} = 0.12$), while all together (all points in Figure 5) have an RMSE ($RMSE_{all}$) of 73 t/ha (normalized $RMSE_{all} = 0.15$).

We also tested a third model version ('disturbed scenario with constant mortality'), in which mortality was kept constant throughout the Amazon (Supporting Information Figure S6). In this scenario, mean AGB is lower, at 199 t/ha, and model performance is weaker, with $R^2 = 0.37$ (Supporting Information Figure S7). This model version does not reach AGB values > 350 t/ha (Supporting Information Figure S8).

The forest model delivers additional forest attributes, such as basal area, tree densities or stem size distributions. Figure 6a (left) shows the spatial distribution of basal area (stem diameter > 10 cm) within the Amazon rain forest, with a mean of 26 m^2/ha and a range between 0 and 48 m^2/ha [relative frequency distribution Figure 6a (right)]. Tree densities [Figure 6b (right)] range between 0 and 920 stems/ha (mean is 484 stems/ha). Figure 6c shows the stem diameter distribution for the entire Amazon rain forest.

4 | DISCUSSION

The estimated AGB varies between 20 and 490 t/ha across the Amazon. This range is a result of a new regionalization approach and the combination of ground data, a remote sensing product and a forest gap model. In the following sections, we discuss the potentials and limitations of combining such information.

4.1 | The regionalization approach

We developed a regionalization approach to transfer the local forest model to the regional scale. In this approach, we analysed the potential drivers for biomass variations in the Amazon. Studies agree that mortality rates drive the spatial variation of AGB within the Amazon rain forest (Castanho et al., 2013; Delbart et al., 2010; Galbraith et al., 2013; Malhi et al., 2015). We tested 40 relationships between mortality rates and environmental factors (Supporting Information Tables S4 and S5). We obtained the best results with precipitation and clay fraction as a proxy for mortality (regarding standard error and R^2). Previous studies support the assumption that a combination of climatic and soil physical conditions could drive turnover rates in the Amazon (de Castilho et al., 2006; Malhi et al., 2006, 2015; Quesada et al., 2012). We detected a decrease of mortality with increasing clay fraction. This relationship might arise from the fact that water retention is higher in clay-rich soils, as hydraulic conductivity decreases with clay fraction (Maidment, 1993). This means that a higher clay fraction compensates, in part, the influence of dry periods on mortality in our forest model.

We developed a regionalization method that quantifies the spatial variation of mortality via a geostatistical approach. A logical next step would be to integrate a soil water module into the forest model. Simulating at monthly time steps might detect potential stress-induced mortality events during dry seasons. This could be an essential step for potential studies exploring the impact of climate change scenarios. However, the parameterization of a root zone soil water module for the entire Amazon is challenging and requires further intensive studies.

4.2 | Distribution of AGB in the Amazon rain forest

The simulated AGB patterns across the Amazon rain forest (Figure 3) are mainly driven by two factors: (a) the variation of forest dynamics because of regionally variable mortality rates; and (b) the variation in forest states defined by the canopy height map. The stem mortality rates influence local forest dynamics by including small-scale disturbances attributable to tree fall. Hence, different mortality rates cause different tree species compositions, which result in a spatial variation of biomass throughout the Amazon rain forest (Figure 2). Simulated mean AGB in climax stage varies between 140 and 366 t/ha ('undisturbed scenario'; Figure 4). This range is similar to old-growth inventories summarized by Malhi et al. (2006). Our simulation result of potential biomass (Supporting Information Figure S3) shows similar patterns in the east and south to those of Malhi et al. (2006). However, the forest model produces higher values in the north-western regions owing to high mean precipitation resulting in low mortality rates (Supporting Information Figure S2).

Large-scale disturbances are reflected in the canopy height map of Simard et al. (2011). Canopy heights are lower in flooded regions along the Amazon river compared with old-growth terra firme stands. Pioneer trees prevail in flooded regions (Martinez & Letoan, 2007). Deforested and secondary forest stands also occur along the 'arc of deforestation' (Nogueira, Fearnside, Nelson, & França, 2007; Nogueira, Nelson, Fearnside, França, & de Oliveira, 2008). Such regions are represented by an earlier successional stage in our forest model and thereby have lower aboveground biomass in our biomass map.

The distribution of AGB in our map resembles in some aspects the distribution of previous AGB maps that are derived from remote sensing data (Avitabile et al., 2016; Saatchi et al., 2011; Supporting Information Figure S9). Differences result from the variation of mortality rates in our forest model that cause differences in forest dynamics. For values > 200 t/ha, AGB values are a bit lower than in the previous maps. In the Western Amazon, where precipitation and clay content are high, our simulations produce higher values. The AGB frequency distributions show the same patterns for values < 200 t/ha.

Johnson et al. (2016) tested several DVGMs to derive AGB maps of the Amazon. The AGB maps of four DGVMs all differ in their patterns and values. DGVMs traditionally capture only undisturbed states of mature forest, whereas forest gap models allow for simulation through all successional states. Thus, the map presented here includes mature forest states, as well as early-to-mid-successional states, by combining the simulation results with height information from remote sensing.

Our simulated map resembles a map created from observations better than the maps produced with the four DGVMs in Johnson et al. (2016). With our approach, we obtain high simulated AGB values in the northeast and lower simulated values towards the southwest. The reason for an AGB gradient in our map lies in the nature of simulating forest structures on the individual tree level with stem mortality rates. Higher mortality rates in the southwest cause stronger dynamics and thereby lower biomass values (Figure 2). In addition, the modelling approach enables the consideration of natural and anthropogenic disturbances by linking simulations to remote sensing data.

4.3 | Limitations of the approach

4.3.1 | Limitations of the forest model

Like every model, forest models include structural uncertainties because of limitations in the knowledge on functional relationships and because of simplifications (e.g., the PFT concept). The comparison of the basal area map (Supporting Information Figure S10) with field data shows an overestimation by 11%, whereas biomass is slightly underestimated (15%). This mismatch is attributable, in part, to the assumption of merely three PFTs for the entire Amazon, for which tree geometry (diameter at breast height–height relationship) parameters are held constant. Additionally, biomass calculations based on allometric relationships of field inventories (Feldpausch et al., 2012) may be regionally adapted and differ from the one used in our simulation (a common tree geometry used for tropical forest simulations based on an allometric function using a form factor as typically used in forestry; Pretzsch, 2010). The comparison of biomass (Figure 5) includes inventory data for secondary and mature forests, whereas the basal area comparison uses only mature forests. The trend, however, between basal area and biomass is similar in inventory data and simulated data (slope in Supporting Information Figure S11). This explains why the pattern of the basal area (Figure 6a) map resembles that of Malhi et al. (2006) regarding high values at the Guiana Shield, at the Amazon river close to the Atlantic ocean, at the Ecuadorian boarder and in the south-west (*c*. 71° W, 12° S). The additional inclusion of younger forests to the validation of basal area would most probably improve the correlation between observed and simulated data (higher R^2; Supporting Information Figure S10).

4.3.2 | Limitations owing to climatological and soil data

Additional limitations arise from input data. Meteorological data (PFFD and precipitation) come from an independent modelling approach at a resolution of 0.5° (Weedon et al., 2014). The clay fraction map arises from an interpolation at 8 km resolution (Wieder et al., 2014). It is difficult to quantify the influence of its spatial resolution on our AGB map. We assume, however, that the input data are reliable to an extent that uncertainties that arise from the input data should be smaller than structural and methodological uncertainties.

4.3.3 | The assumption of canopy height as a proxy for successional states and disturbed forests

This assumption is inspired by a pioneering study that linked canopy height and a forest model to derive biomass for local forests sites in Costa Rica (Hurtt et al., 2004). Taking the large-scale canopy height map as a proxy for successional states has several limitations. First, the proxy is not explicit, because canopy height can be associated with different stem size distributions. The canopy height map does not provide information on forest history (i.e., a forest could be in a state of regrowth after anthropogenic degradation or in a maturing state after a natural disturbance event). Second, we are aware of the fact that the canopy height map provides a proxy only at a resolution of 1 km^2 and does not capture the full spatial height heterogeneity. The canopy height map is a product of discrete recordings by LIDAR that are transferred into a continuous map via a modelling approach (Simard et al., 2011). We relied on those modelled values and assumed that they are representative. It is the best information we have at the moment to identify large-scale successional stages within the Amazon.

It would be interesting to integrate other satellite products into our approach, such as the normalized difference vegetation index (NDVI; Running et al., 2004). In future studies, they could improve estimates of disturbed regions with lower biomass values and lower tree densities, because it is available at high resolution and could be taken as a proxy for leaf area index. However, in dense mature forests, it is known that the NDVI saturates and thus has limited capability to identify spatial variation (Hall et al., 2011; Myneni et al., 2001).

4.3.4 | Uncertainties in field inventory data

Forest inventories can include measurement errors, coordinate uncertainties and unrepresentative sample plots (Saatchi et al., 2015). In addition, inventory data often come from small plots (*c*. 1 ha). At such small scales, biomass can vary strongly (Chambers et al., 2013). The validation of the AGB map (Figure 5) has shown that samples with a sample size $\geq$ 4 ha (critical sample size in Réjou-Méchain et al., 2014) match the 1:1 line better than samples of smaller sizes (normalized RMSE of 0.12 vs. 0.15). In total, mean simulated AGB is 15% lower than mean observed AGB. One reason for this underestimation of inventory values may be the 'bias towards majestic forest stands' for field inventories (Malhi et al., 2002), a bias resulting from preferentially selecting old-growth, gap-free inventory sites.

4.4 | Benefits from linking remote sensing and forest models

Saatchi et al. (2015) listed the following main challenges when estimating AGB in tropical forests: (a) considering diversity in structure, wood density and dynamics and the complexity of allometries; (b) including natural and anthropogenic disturbances; and (c) weak relationships between environmental conditions and biomass. They concluded that ground and remote sensing observations need to be linked to estimate biomass at the large scale. In our study, we additionally integrated an individual-based forest model to estimate the AGB of the Amazon. Forest gap models, in particular FORMIND, are developed to simulate forest structures of highly diverse tropical forests, thus addressing challenges (a) and (b). Calculating forest dynamics at the individual tree level allows for consideration of complex height structure and enables the analysis of forest structures of disturbed and undisturbed sites (Köhler & Huth, 1998). In this respect, forest gap models differ from several dynamic global vegetation models, which handle forest stands as an average individual and are often insufficient to capture detailed structures of tropical forests (Johnson et al., 2016). Furthermore, we also tackled challenge (c) by analysing the influence of local environmental conditions on tree mortality rate.

Bridging the gap between different spatial scales of ground-based observations and remote sensing products with the help of an individual-based forest gap model can provide a better understanding of heterogeneous forest structures. Given that forest gap models

capture the dynamics and states at the individual tree level, maps of various forest attributes (Figure 6; tree density for different tree sizes in Supporting Information Figure S12) at different spatial resolutions can be derived ($\geq$ 0.4 ha for AGB in Figure 3).

The approach presented here sets a foundation for further structural, large-scale analyses on disturbances (e.g., Huth, Drechsler, & Köhler, 2004), secondary forest regrowth (e.g., Poorter et al., 2016), fragmentation (e.g., Pütz et al., 2014) or, with an extended model version, on future climate scenarios (e.g., Rammig et al., 2010).

5 | CONCLUSION

Individual-based forest gap models simulate forest dynamics throughout all successional states. By capturing forest structures at small scales, they are able to fill a gap between large-scale vegetation modelling (such as DGVMs), remote sensing products and ground observations. With our approach, we perceive the opportunity to complement the linkage between ground and remote-sensing observations (Saatchi et al., 2011). The individual-based forest gap model represents a tool with spatially explicit information on forest structures and dynamics. The validation with field inventories has shown that forest structure, in terms of species composition and forest height, has a strong influence on the spatial variation of biomass in the Amazon rain forest. The approach opens new doors to the analysis of highly diverse, large-scale forest structures of the Amazon rain forest concerning carbon fluxes, disturbances and climate change scenarios. In combination with products of future remote sensing missions (e.g., European Space Agency (ESA) Biomass, Global Ecosystem Dynamics Investigation Lidar (GEDI) or proposed Tandem-L; Moreira et al., 2015), better insights into large-scale structures and dynamics of tropical forests will be feasible.

DATA ACESSIBITITY

Maps of AGB, basal area and stem number (tiff and netcdf format) are available online on http://formind.org/amazon/. The FORMIND model (executable) is freely available on http://formind.org/downloads/.

ORCID

Edna Rödig http://orcid.org/0000-0002-6248-8844

ACKNOWLEDGMENTS

This study was supported by the Helmholtz-Alliance Remote Sensing and Earth System Dynamics. E.R. was kindly supported by the Helmholtz Impulse and Networking Fund through the Helmholtz Interdisciplinary Graduate School for Environmental Research (HIGRADE). We thank Rico Fischer, Franziska Taubert, Sebastian Paulick, Michael Müller, Matthias Zink and Juliane Mai for helpful discussions and technical support. We greatly appreciate the constructive and thoughtful comments of the referees and the editor.

REFERENCES

Avitabile, V., Herold, M., Heuvelink, G. B. M., Lewis, S. L., Phillips, O. L., Asner, G. P., ... Willcock, S. (2016). An integrated pan-tropical biomass map using multiple reference datasets. *Global Change Biology*, *22*, 1406–1420.

Baccini, A., Goetz, S. J., Walker, W. S., Laporte, N. T., Sun, M., Sulla-Menashe, D., ... Houghton, R. A. (2012). Estimated carbon dioxide emissions from tropical deforestation improved by carbon-density maps. *Nature Climate Change*, *2*, 182–185.

Blöschl, G., & Sivapalan, M. (1995). Scale issues in hydrological modelling: A review. *Hydrological Processes*, *9*, 251–290.

Botkin, D. B., Janak, J. F., & Wallis, J. R. (1972). Some ecological consequences of a computer model of forest growth. *Journal of Ecology*, *60*, 849–872.

Brondizio, E. S., & Moran, E. F. (2009). *LBA-ECO LC-09 vegetation composition and structure in the Brazilian Amazon: 1992–1995. Data set*. Oak Ridge, TN: Oak Ridge National Laboratory Distributed Active Archive Center. Retrieved from http://daac.ornl.gov

Bugmann, H. (2001). A review of forest gap models. *Climatic Change*, *51*, 259–305.

Castanho, A. D. A., Coe, M. T., Costa, M. H., Malhi, Y., Galbraith, D., & Quesada, C. A. (2013). Improving simulated Amazon forest biomass and productivity by including spatial variation in biophysical parameters. *Biogeosciences*, *10*, 2255–2272.

CDO. (2015). *CDO 2015: Climate Data Operators*. Retrieved from http://www.mpimet.mpg.de/cdo

Chambers, J. Q., Negron-Juarez, R. I., Marra, D. M., Di Vittorio, A., Tews, J., Roberts, D., ... Higuchi, N. (2013). The steady-state mosaic of disturbance and succession across an old-growth Central Amazon forest landscape. *Proceedings of the National Academy of Sciences USA*, *110*, 3949–3954.

Chave, J. J. J., Condit, R., Aguilar, S., Hernandez, A., Lao, S., & Perez, R. (2004). Error propagation and scaling for tropical forest biomass estimates. *Philosophical Transactions of the Royal Society B: Biological Sciences*, *359*, 409–420.

de Castilho, C. V., Magnusson, W. E., de Araújo, R. N. O., Luizão, R. C. C., Luizão, F. J., Lima, A. P., & Higuchi, N. (2006). Variation in aboveground tree live biomass in a central Amazonian forest: Effects of soil and topography. *Forest Ecology and Management*, *234*, 85–96.

Delbart, N., Ciais, P., Chave, J., Viovy, N., Malhi, Y., & Le Toan, T. (2010). Mortality as a key driver of the spatial distribution of aboveground biomass in Amazonian forest: Results from a dynamic vegetation model. *Biogeosciences*, *7*, 3027–3039.

Dubayah, R. O., Sheldon, S. L., Clark, D. B., Hofton, M. A., Blair, J. B., Hurtt, G. C., & Chazdon, R. L. (2010). Estimation of tropical forest height and biomass dynamics using lidar remote sensing at la Selva, Costa Rica. *Journal of Geophysical Research: Biogeosciences*, *115*, 1–17.

Feldpausch, T. R., Banin, L., Phillips, O. L., Baker, T. R., Lewis, S. L., Quesada, C. A., ... Lloyd, J. (2011). Height-diameter allometry of tropical forest trees. *Biogeosciences*, *8*, 1081–1106.

Feldpausch, T. R., Lloyd, J., Lewis, S. L., Brienen, R. J. W., Gloor, M., Monteagudo Mendoza, A., ... Phillips, O. L. (2012). Tree height integrated into pantropical forest biomass estimates. *Biogeosciences*, *9*, 3381–3403.

Fischer, R., Bohn, F., Dantas de Paula, M., Dislich, C., Groeneveld, J., Gutiérrez, A. G., ... Huth, A. (2016). Lessons learned from applying a forest gap model to understand ecosystem and carbon dynamics of complex tropical forests. *Ecological Modelling*, *326*, 124–133.

Flügel, W.-A. (1995). Delineating hydrological response units by geographical information system analyses for regional hydrological

modelling using PRMS/MMS in the drainage basin of the River Bröl, Germany. *Hydrological Processes*, *9*, 423–436.

Galbraith, D., Malhi, Y., Affum-Baffoe, K., Castanho, A. D., Doughty, C. E., Fisher, R. A., … Lloyd, J. (2013). Residence times of woody biomass in tropical forests. *Plant Ecology and Diversity*, *6*, 139–157.

Hall, F. G., Bergen, K., Blair, J. B., Dubayah, R., Houghton, R., Hurtt, G., … Wickland, D. (2011). Characterizing 3D vegetation structure from space: Mission requirements. *Remote Sensing of Environment*, *115*, 2753–2775.

Hansen, M. C., Stehman, S. V., & Potapov, P. V. (2010). Quantification of global gross forest cover loss. *Proceedings of the National Academy of Sciences USA*, *107*, 8650–8655.

Hofhansl, F., Andersen, K. M., Fleischer, K., Fuchslueger, L., Rammig, A., Schaap, K. J., … Lapola, D. M. (2016). Amazon forest ecosystem responses to elevated atmospheric CO_2 and alterations in nutrient availability: Filling the gaps with model-experiment integration. *Frontiers in Earth Science*, *4*, 1–9.

Houghton, R. A., Lawrence, K. T., Hackler, J. L., & Brown, S. (2001). The spatial distribution of forest biomass in the Brazilian Amazon: A comparison of estimates. *Global Change Biology*, *7*, 731–746.

Huntingford, C., Fisher, R. A., Mercado, L., Booth, B. B. B., Sitch, S., Harris, P. P., … Moorcroft, P. (2008). Towards quantifying uncertainty in predictions of Amazon 'dieback'. *Philosophical Transactions of the Royal Society B: Biological Sciences*, *363*, 1857–1864.

Hurtt, G. C., Dubayah, R., Drake, J., Moorcroft, P. R., Pacala, S. W., Blair, J. B., & Fearon, M. G. (2004). Beyond potential vegetation: Combining lidar data and a height-structured model for carbon studies. *Ecological Applications*, *14*, 873–883.

Huth, A., Drechsler, M., & Köhler, P. (2004). Multicriteria evaluation of simulated logging scenarios in a tropical rain forest. *Journal of Environmental Management*, *71*, 321–333.

Johnson, M. O., Galbraith, D., Gloor, E., De Deurwaerder, H., Guimberteau, M., Rammig, A., … Baker, T. R. (2016). Variation in stem mortality rates determines patterns of aboveground biomass in Amazonian forests: Implications for dynamic global vegetation models. *Global Change Biology*, *22*, 3996–4013.

Köhler, P., & Huth, A. (1998). The effects of tree species grouping in tropical rainforest modelling: Simulations with the individual-based model Formind. *Ecological Modelling*, *109*, 301–321.

Köhler, P., & Huth, A. (2004). Simulating growth dynamics in a South-East Asian rainforest threatened by recruitment shortage and tree harvesting. *Climatic Change*, *67*, 95–117.

Kunert, N., Aparecido, L. M. T., Higuchi, N., Santos, J., & Dos Trumbore, S. (2015). Higher tree transpiration due to road-associated edge effects in a tropical moist lowland forest. *Agricultural and Forest Meteorology*, *213*, 183–192.

Le Quéré, C., Andrew, R. M., Canadell, J. G., Sitch, S., Korsbakken, J. I., Peters, G. P., … Zaehle, S. (2016). Global Carbon Budget 2016. *Earth System Science Data*, *8*, 605–649.

Lehmann, S., & Huth, A. (2015). Fast calibration of a dynamic vegetation model with minimum observation data. *Ecological Modelling*, *301*, 98–105.

Lopez-Gonzalez, G., Lewis, S. L., Burkitt, M. & Phillips, O. L. (2011). Forest-Plots.net: A web application and research tool to manage and analyse tropical forest plot data. *Journal of Vegetation Science*, *22*, 610–613.

Lopez-Gonzalez, G., Mitchard, E. T. A., Feldpausch, T. R., Brienen, R. J. W., Monteagudo, A., Baker, T. R., … Phillips, O. L. (2014). *Amazon forest biomass measured in inventory plots*. Plot Data from "Markedly divergent estimates of Amazon forest carbon density from ground plots and satellites. Retrieved from http://www.forestplots.net

Maidment, D. (1993). *Handbook of hydrology*. New York, NY: McGraw Hill Inc.

Malhi, Y., Doughty, C. E., Goldsmith, G. R., Metcalfe, D. B., Girardin, C. A J., Marthews, T. R., … Phillips, O. L. (2015). The linkages between photosynthesis, productivity, growth and biomass in lowland Amazonian forests. *Global Change Biology*, *21*, 2283–2295.

Malhi, Y., Phillips, O. L., Lloyd, J., Baker, T., Wright, J., Almeida, S., … Vinceti, B. (2002). An international network to monitor the structure, composition and dynamics of Amazonian forests (RAINFOR). *Journal of Vegetation Science*, *13*, 439.

Malhi, Y., Wood, D., Baker, T. R., Wright, J., Phillips, O. L., Cochrane, T., … Vinceti, B. (2006). The regional variation of aboveground live biomass in old-growth Amazonian forests. *Global Change Biology*, *12*, 1107–1138.

Martinez, J., & Letoan, T. (2007). Mapping of flood dynamics and spatial distribution of vegetation in the Amazon floodplain using multitemporal SAR data. *Remote Sensing of Environment*, *108*, 209–223.

Marvin, D. C., Asner, G. P., Knapp, D. E., Anderson, C. B., Martin, R. E., Sinca, F., & Tupayachi, R. (2014). Amazonian landscapes and the bias in field studies of forest structure and biomass. *Proceedings of the National Academy of Sciences USA*, *111*, E5224–E5232.

Mitchard, E. T. A., Feldpausch, T. R., Brienen, R. J. W., Lopez-Gonzalez, G., Monteagudo, A., Baker, T. R., … Phillips, O. L. (2014). Markedly divergent estimates of Amazon forest carbon density from ground plots and satellites. *Global Ecology and Biogeography*, *23*, 935–946.

Moreira, A., Krieger, G., Hajnsek, I., Papathanassiou, K., Younis, M., Lopez-Dekker, P., … Parizzi, A. (2015). A highly innovative bistatic SAR mission for global observation of dynamic processes on the earth's surface. *IEEE Geoscience and Remote Sensing Magazine*, *3*, 8–23.

Myneni, R. B., Dong, J., Tucker, C. J., Kaufmann, R. K., Kauppi, P. E., Liski, J., … Hughes, M. K. (2001). A large carbon sink in the woody biomass of Northern forests. *Proceedings of the National Academy of Sciences USA*, *98*, 14784–14789.

Nogueira, E. M., Fearnside, P. M., Nelson, B. W., & França, M. B. (2007). Wood density in forests of Brazil's 'arc of deforestation': Implications for biomass and flux of carbon from land-use change in Amazonia. *Forest Ecology and Management*, *248*, 119–135.

Nogueira, E. M., Nelson, B. W., Fearnside, P. M., França, M. B., & de Oliveira, Á. C. A. (2008). Tree height in Brazil's 'arc of deforestation': Shorter trees in south and southwest Amazonia imply lower biomass. *Forest Ecology and Management*, *255*, 2963–2972.

Poorter, L., Bongers, F., Aide, T. M., Almeyda Zambrano, A. M., Balvanera, P., Becknell, J. M., … Rozendaal, D. M. A. (2016). Biomass resilience of Neotropical secondary forests. *Nature*, *530*, 211–214.

Poorter, L., van der Sande, M. T., Thompson, J., Arets, E. J. M. M., Alarcón, A., Álvarez-Sánchez, J., … Peña-Claros, M. (2015). Diversity enhances carbon storage in tropical forests. *Global Ecology and Biogeography*, *24*, 1314–1328.

Pretzsch, H. (2010). *Forest dynamics, growth and yield*. Berlin, Heidelberg: Springer Berlin Heidelberg.

Pütz, S., Groeneveld, J., Henle, K., Knogge, C., Martensen, A. C., Metz, M., … Huth, A. (2014). Long-term carbon loss in fragmented Neotropical forests. *Nature Communications*, *5*, 5037.

Quesada, C. A., Phillips, O. L., Schwarz, M., Czimczik, C. I., Baker, T. R., Patiño, S., … Lloyd, J. (2012). Basin-wide variations in Amazon forest structure and function are mediated by both soils and climate. *Biogeosciences*, *9*, 2203–2246.

Rammig, A., Jupp, T., Thonicke, K., Tietjen, B., Heinke, J., Ostberg, S., … Cox, P. (2010). Estimating the risk of Amazonian forest dieback. *New Phytologist*, *187*, 694–706.

Ranson, K. J., Sun, G., Knox, R. G., Levine, E. R., Weishampel, J. F., & Fifer, S. T. (2001). Northern forest ecosystem dynamics using coupled models and remote sensing. *Remote Sensing of Environment*, *75*, 291–302.

Réjou-Méchain, M., Muller-Landau, H. C., Detto, M., Thomas, S. C., Le Toan, T., Saatchi, S. S., … Chave, J. (2014). Local spatial structure of forest biomass and its consequences for remote sensing of carbon stocks. *Biogeosciences*, *11*, 6827–6840.

Running, S. W., Nemani, R. R., Heinsch, F. A., Zhao, M., Reeves, M., & Hashimoto, H. (2004). A Continuous satellite-derived measure of global terrestrial primary production. *BioScience*, *54*, 547.

Saatchi, S., Mascaro, J., Xu, L., Keller, M., Yang, Y., Duffy, P., … Schimel, D. (2015). Seeing the forest beyond the trees. *Global Ecology and Biogeography*, *24*, 606–610.

Saatchi, S. S., Harris, N. L., Brown, S., Lefsky, M., Mitchard, ET. A., Salas, W., … Morel, A. (2011). Benchmark map of forest carbon stocks in tropical regions across three continents. *Proceedings of the National Academy of Sciences USA*, *108*, 9899–9904.

Saatchi, S. S., Houghton, R. A., Dos Santos Alvalá, R. C., Soares, J. V., & Yu, Y. (2007). Distribution of aboveground live biomass in the Amazon basin. *Global Change Biology*, *13*, 816–837.

Samaniego, L., Kumar, R., & Attinger, S. (2010). Multiscale parameter regionalization of a grid-based hydrologic model at the mesoscale. *Water Resources Research*, *46*, W05523.

Shugart, H. H. (1984). *A theory of forest dynamics*. Caldwell, NJ: The Blackburn Press.

Shugart, H. H., Asner, G. P., Fischer, R., Huth, A., Knapp, N., Le Toan, T., & Shuman, J. K. (2015). Computer and remote-sensing infrastructure to enhance large-scale testing of individual-based forest models. *Frontiers in Ecology and the Environment*, *13*, 503–511.

Simard, M., Pinto, N., Fisher, J. B., & Baccini, A. (2011). Mapping forest canopy height globally with spaceborne lidar. *Journal of Geophysical Research*, *116*, G04021.

Sitch, S., Smith, B., Prentice, I. C., Arneth, A., Bondeau, A., Cramer, W., … Venevsky, S. (2003). Evaluation of ecosystem dynamics, plant geography and terrestrial carbon cycling in the LPJ dynamic global vegetation model. *Global Change Biology*, *9*, 161–185.

Smith, B., Prentice, I. C., & Sykes, M. T. (2001). Representation of vegetation dynamics in the modelling of terrestrial ecosystems: Comparing two contrasting approaches within European climate space. *Global Ecology and Biogeography*, *10*, 621–637.

van der Werf, G. R., Morton, D. C., DeFries, R. S., Olivier, J. G. J., Kasibhatla, P. S., Jackson, R. B., … Randerson, J. T. (2009). CO_2 emissions from forest loss. *Nature Geoscience*, *2*, 737–738.

Weedon, G. P., Balsamo, G., Bellouin, N., Gomes, S., Best, M. J., & Viterbo, P. (2014). The WFDEI meteorological forcing data set: WATCH forcing data methodology applied to ERA-Interim reanalysis data. *Water Resources Research*, *50*, 7505–7514.

Wieder, W. R., Boehnert, J., Bonan, G. B., & Langseth, M. (2014). *Regridded harmonized world soil database v1.2*. *Data set*. Oak Ridge, TN: Oak Ridge National Laboratory Distributed Active Archive Center. Retrieved from http://daac.ornl.gov

BIOSKETCH

Edna Rödig is a PhD student at the Helmholtz-Centre for Environmental Research, Germany. She is part of a research team that works on the simulation of tropical forests with an individual-based forest model. Her main research focus is upscaling the forest model to the large scale (e.g., the Amazon rain forest). All authors combine their interest in linking remote sensing products with vegetation modelling and improving large-scale simulations.

SUPPORTING INFORMATION

Additional Supporting Information may be found online in the supporting information tab for this article.

How to cite this article: Rödig E, Cuntz M, Heinke J, Rammig A, Huth A. Spatial heterogeneity of biomass and forest structure of the Amazon rain forest: Linking remote sensing, forest modelling and field inventory. *Global Ecol Biogeogr*. 2017;26:1292–1302. https://doi.org/10.1111/geb.12639